

Gammasphere at ATLAS: Physics at the Limits

R.V.F. Janssens ^a

^aPhysics Division, Argonne National Laboratory, Argonne, Illinois 60439, U.S.A.

The Gammasphere array of Compton-suppressed spectrometers has just completed a cycle of experiments at the ATLAS accelerator at Argonne National Laboratory. A majority of experiments studied the properties of nuclei at the very limits of stability in various regions of the periodic table. This contribution discusses through a few examples the major physics issues that have been investigated.

1. INTRODUCTION

The Gammasphere array [1] was moved from the 88-Inch cyclotron at Lawrence Berkeley National Laboratory, where it was originally assembled, to the ATLAS superconducting linear Accelerator at Argonne National Laboratory with the aim of directing the power of the instrument towards exotic nuclei far from stability. This goal was made possible in large part by the coupling of the device with the Fragment Mass Analyzer (FMA) [2], an instrument tailored towards the detection and identification of evaporation residues in the presence of large backgrounds due to other processes. In addition, the wide range of beams available from the ATLAS accelerator and the exceptional timing characteristics made many novel uses of Gammasphere possible.

During its 26 months stay at Argonne, Gammasphere took data for a total of more than 11,000 hours for 101 experiments. It would clearly be impossible to summarize here most of what has been accomplished. Rather, this presentation focuses on a few examples which can be viewed as milestones in the exploration of nuclei at the very limits of stability. In ^{253,254}No discrete line spectroscopy as well as calorimetry measurements were performed for the first time. The results show these heavy, fissile nuclei to be more stable against rotation than had previously been thought. Extensive measurements were carried out beyond the proton drip-line, transforming this area of research from the qualitative mapping of the location of the drip-line into the quantitative measurement of the shapes and quantum numbers of levels in these marginally bound systems. Experiments in light nuclei focussed particularly on the $N=Z$ line and addressed the role of pairing correlations. In addition, new data for nuclei with mass $A < 40$ have provided an opportunity to compare predictions based on the spherical shell model and on the Nilsson-Strutinsky description with cranking with the goal of gathering valuable insight into the microscopic degrees of freedom contributing to rotational motion.

2. SHELL STABILIZED HIGH-Z NUCLEI

2.1. Yrast Spectroscopy and Deformation of $^{253,254}\text{No}$

The heaviest nuclei, with $Z > 100$, are at the limit of Coulomb instability, and would be unstable against spontaneous fission but for a large shell-correction energy, which leads to additional binding and creates a sizable fission barrier. The relative stability of these very heavy elements is a striking manifestation of shell structure in nuclei. Its importance was highlighted again recently with reports of the detection of elements 114, 116 and 118 [3,4]. Theoretical studies have indicated that these shell effects lead to an island of spherical superheavy elements [5] based on doubly closed neutron ($N=184$) and proton ($Z=114$) shells. In contrast, the observed stability of lighter transfermium nuclei with Z up to 112 is explained [6] by invoking the ability of these nuclei to deform, e.g. the shell-correction energy is the largest for a sizable quadrupole deformation with contributions from higher order multipole moments.

Two isotopes of element 102, ^{254}No and ^{253}No have been studied with Gammasphere and the FMA using the Recoil Decay Tagging technique (RDT) where prompt gamma radiation measured at the target position is correlated with (i) the specific mass/charge ratio of a residue (as inferred from the position at which the recoil crosses the FMA focal plane) and (ii) the subsequent characteristic alpha decay (measured with a Double-Sided Si Strip detector). A detailed account of these experiments can be found in Refs. [7] and [8].

Fig. 1 compares the γ spectra obtained with the $^{208}\text{Pb}(^{48}\text{Ca}, 2n)^{254}\text{No}$ reaction at beam energies of 215 and 219 MeV. Transitions from higher-spin members of the groundstate band are clearly enhanced at the higher bombarding energy, and the decay of levels with spin as high as $20\hbar$ has been observed. At both energies, the high efficiency of Gammasphere enabled to verify coincidence relationships between the transitions despite the small production cross sections (a few μb). The identification of a rotational band immediately establishes that ^{254}No is a deformed nucleus. An inset in Fig. 1 presents the $\mathfrak{I}^{(1)}$ moment of inertia as a function of the rotational frequency. The spins of the emitting states and the energies of the lowest levels, which were not detected because they decay almost entirely by internal conversion, were deduced using fits to this smooth curve based on the Harris parametrization. Furthermore, using expressions relating the 2^+ level energy with the $B(E2)$ values of rotors and those relating the $B(E2)$, quadrupole moment, and deformation, a quadrupole deformation parameter of $\beta = 0.27(2)$ was deduced for ^{254}No (see Ref. [7] for details). This value is in agreement with a value of 0.25 given by different macroscopic model calculations [9], and with values of 0.27 and 0.26 from HFB [10] and relativistic mean field [11] calculations, respectively. The moment of inertia is also an important quantity for theory to describe as it is sensitive to the single-particle energies and pairing. HFB calculations of this quantity with both the SLy4 [12] and the Gogny [13] forces have recently become available. They reproduce the evolution of the moment of inertia with spin satisfactorily and assign the smooth increase with frequency to the gradual alignment of $i_{13/2}$ protons and $j_{15/2}$ neutrons

More recently, the nucleus ^{253}No was studied with the $^{207}\text{Pb}(^{48}\text{Ca}, 2n)$ at 219 MeV with the objective of providing more information on the behavior of neutron orbitals

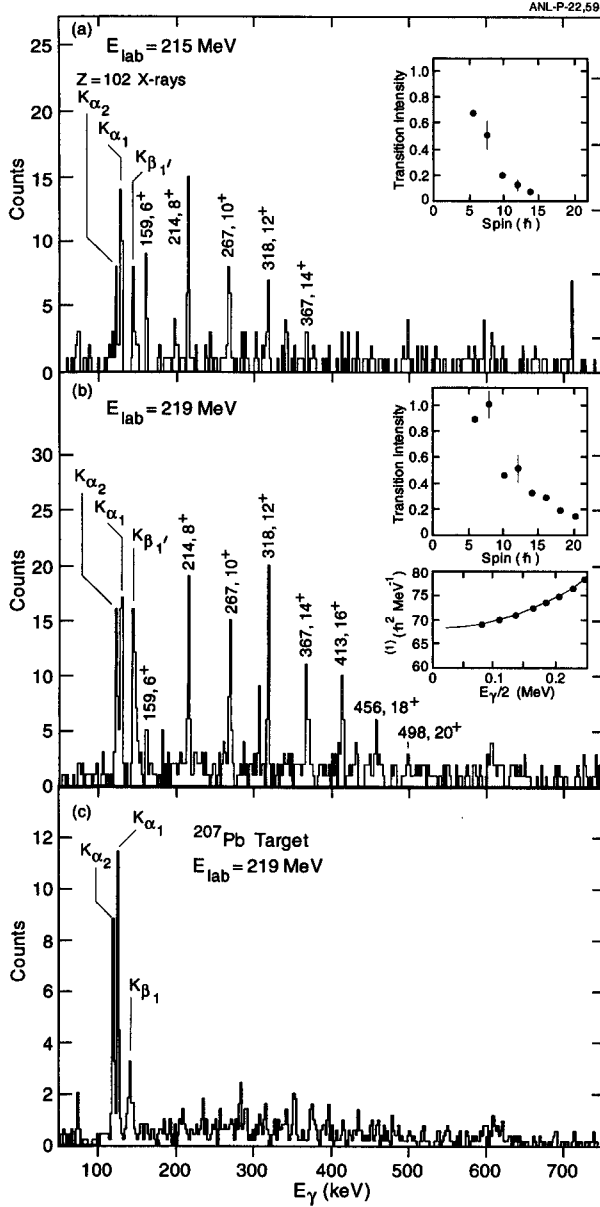


Figure 1. (a) and (b): ^{254}No spectra obtained at two beam energies. The transitions are labeled by their energies and initial spins. The intensity profiles are given as insets. A second inset in (b) shows the evolution with frequency of the moment of inertia. The spectrum obtained for ^{253}No is shown in panel (c). See Refs. [7,8] for further details.

located in the vicinity of the Fermi surface. The results of this experiment are still preliminary. As can be seen in the bottom panel of Fig. 1, the spectrum measured in coincidence with $A=253$ residues is quite different from those presented for ^{254}No : the No x-rays dominate the spectrum and an appreciable number of weaker γ transitions are present at higher energies. These observations should not be viewed as a surprise. Electron-capture decay measurements into the isotone ^{249}Cf [14] and alpha decay studies into ^{253}No itself [15] have shown that a number of neutron excitations occur within ~ 500 keV of the groundstate. Hence, several collective band structures can be expected to receive appreciable population in the reaction. In addition, the deexcitation of the states in these bands will be characterized by a competition between M1 ($I \rightarrow I-1$) and E2 ($I \rightarrow I-2$) transitions. The M1 transitions will be highly converted, as will the lowest energy E2 γ rays. The competition between the two deexcitation modes depends on the intrinsic structure of the neutron orbitals and only excitations built on orbitals where the $B(M1)$ reduced probabilities are relatively small can be expected to result in a rotational cascade dominated by E2 transitions with sufficient intensity to be detected by Gammasphere. A search for such structures has resulted in a positive signal. The analysis is, however, still in an early stage and more work is needed before a firm assignment can be made.

2.2. Entry Distribution, Fission Barrier, and Formation Mechanism

Taking advantage of the fact that Gammasphere covers most of the 4π solid angle around the target, the entry distribution in angular momentum and excitation energy for the formation of ^{254}No was determined at both beam energies from the number of detector modules that fired and the total energy emitted by γ radiation in each event. The technique and the results are discussed in detail in Ref. [8]. The entry distributions are compared in Fig. 2 for the two beam energies. The one-dimensional spin and excitation energy distributions are given as well.

At the lower beam energy, it is the maximum allowable energy after neutron emission that imposes a $16\hbar$ limit on the angular momentum and not the fission barrier. At the higher energy, states up to $22\hbar$ and an excitation energy $E^* = 8.5$ MeV are populated. Clearly, ^{254}No can survive against fission up to these limits. Gamma decay to the ground state originates from the entry distribution, implying successful competition against fission. As described in detail in Ref. [8], these data provide a lower bound on the fission barrier B_f : even at high spin $B_f \geq 5$ MeV, a value which in turn corresponds to a constraint on the shell energy of $E_{\text{shell}} \geq 4$ MeV for spin values $I = 12-22\hbar$. The measured entry distribution contradicts the hypothesis that the shell-correction energy decreases to $1/e$ of its zero spin value at spin 15 [16], and is in agreement with a much smaller decrease with angular momentum obtained in the HFB calculations of Refs. [12,13]. An unexpected feature of the entry distributions of Fig. 2 is the sharp tilt angle with respect to the yrast line. This is due, at least in part, to the small excitation energy of the low-spin entry states, which appears to be a distinct component of the distribution. The deviation of the entry distribution from the line representing E^*_{max} gives the energy removed by the two neutrons, and the evaporation residues with low partial waves seem to be associated with unusually energetic neutrons. On the other hand, at higher spin ($I \geq 14\hbar$) the entry distributions above the yrast line are more usual. Hence, there is a hint of at least two mechanisms in the formation of these very heavy nuclei: a nor-

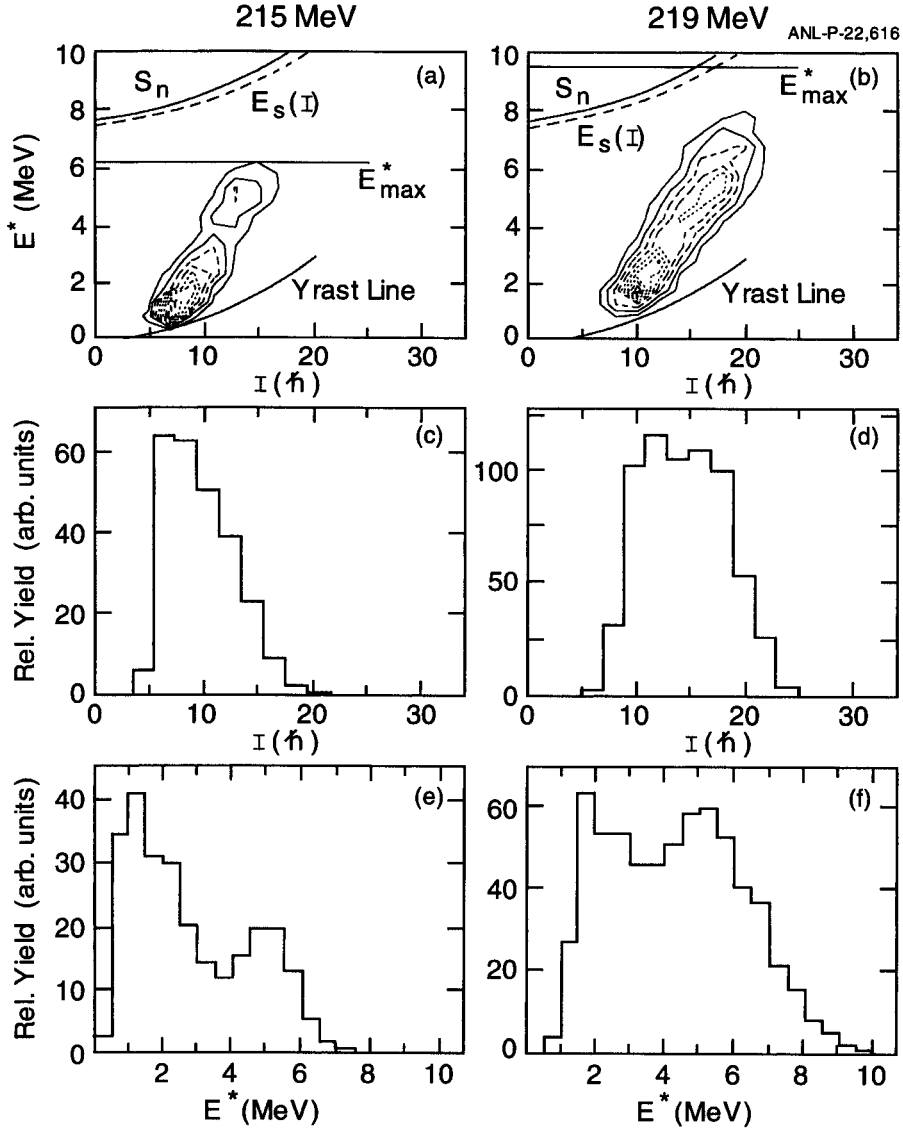


Figure 2. Contour plots of the ^{254}No entry distributions in spin and excitation energy and their projections at the two beam energies (left-215 MeV, right-219 MeV). The measured yrast line, the neutron-separation energy S_n , a theoretical saddle-point energy $E_s(I)$ and the maximum possible energy in ^{254}No ($E_{\text{max}}^* = E_{CN} - S_{n1} - S_{n2}$) are indicated. Taken from Ref. [8].

mal, statistical one responsible for high spin formation and another one with emission of higher-energy (perhaps preequilibrium) neutrons, which is important at lower spins. It is worth noting that the preliminary analysis of the ^{253}No entry distribution confirms the conclusions given here for ^{254}No .

3. LEVEL STRUCTURE IN A DEFORMED PROTON-EMITTER

By now, great progress has been made in delineating the proton drip line for nuclei located between Sn and Pb, and it has been realized that proton radioactivity can be used as a spectroscopic tool providing vital information about the emitting states such as spin, parity, spectroscopic factors and orbital assignments [17]. Recently, anomalous decay rates have been observed in ^{131}Eu and ^{141}Ho [18] which were interpreted as evidence for large deformation. These two nuclei have been reinvestigated with Gammasphere and the FMA. Here, the results for ^{141}Ho are briefly discussed.

The RDT technique was used to identify transitions in ^{141}Ho with the $^{54}\text{Fe}(^{92}\text{Mo}, p4n)$ reaction at 502 MeV [19]. Level structures built on the two p-emitting states in this nucleus have been established. The relevant level scheme is presented in Fig. 3, where the dynamic moments of inertia are also given as a function of rotational frequency for the two sequences. It is worth noting that the cross section for the production of the isomer is only 50 nb.

Based on the work of Ref. [18], the ^{141}Ho ground state was associated with the $7/2^-$ [523] orbital of $h_{11/2}$ parentage and the associated deformation was determined to be $\beta_2 = 0.29(3)$. From Fig. 3 it is clear that the rotational character of the sequence built on this state confirms that this proton emitter is deformed. The $\mathfrak{I}^{(2)}$ moment of inertia for this band shows little variation with rotational frequency, an observation which is in line with the $h_{11/2}$ assignment to this band. Indeed, in nuclei of this region, the first crossing is due to the alignment of a pair of $h_{11/2}$ protons and has been observed to occur at a frequency of ~ 0.25 MeV. This alignment is blocked in a nucleus where the single proton occupies this $h_{11/2}$ orbital. As explained in detail in Ref. [19], a fit to the dynamic moment of inertia yields a value of the deformation of $\beta_2 = 0.25(4)$, i.e. slightly smaller, but in qualitative agreement with the value inferred from proton decay. The band built on the $1/2^+$ [411] isomer (of $s_{1/2}$ parentage) is characterized by a $\mathfrak{I}^{(2)}$ moment which rises sharply with frequency. This too is consistent with the proposed assignment as the $h_{11/2}$ proton alignment is no longer blocked in this instance.

The results discussed thus far are in agreement with those obtained from proton decay. Yet, the data contain a surprise. Indeed, for an axially symmetric ^{141}Ho nucleus, the collective band built on the $7/2^-$ [523] orbital would be expected to correspond to a strongly coupled sequence of the type $(7/2^- \leftarrow 9/2^- \leftarrow 11/2^- \leftarrow 13/2^- \leftarrow 15/2^- \dots)$. From Fig. 3, it appears that (i) only the $9/2^-$ and $13/2^-$ members of the so-called signature partner band are visible and that (ii) there is significant signature splitting. Cranked shell model calculations show that such a splitting can only be achieved by postulating a significant degree of triaxiality: $\gamma \sim -20^\circ$. So far, this degree of freedom has not been considered by theory and its impact on the calculation of decay rates remains to be evaluated.

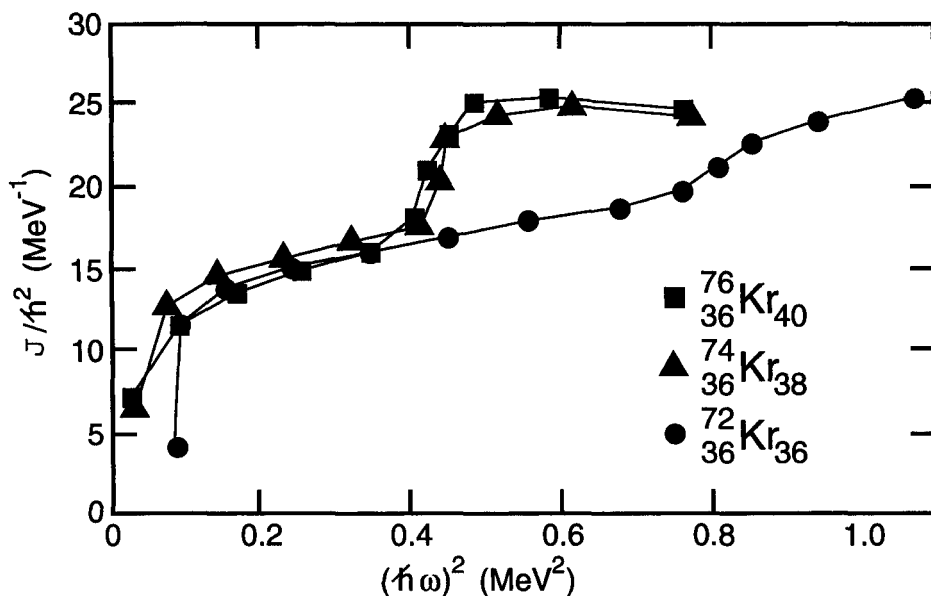


Figure 4. Comparison of the moments of inertia as a function of rotational frequency in the even-even $^{72-76}\text{Kr}$. Taken from Ref. [22].

measured binding energies [23]. Another fingerprint for $S=1$, $T=0$ p-n pairing that has been suggested concerns the high-spin properties of $N = Z$ nuclei [24]. Specifically, the additional contribution to pairing has been predicted to delay particle alignments along the yrast line.

Figure 4 compares the moments of inertia of $^{74,76}\text{Kr}$ [25,26] with that of the $N = Z$ nucleus ^{72}Kr [22]. The data on the latter nucleus were obtained with the $^{40}\text{Ca}(^{40}\text{Ca}, 2\alpha)$ reaction at 160 MeV using Gammasphere in conjunction with Microball, a charged-particle array of CsI detectors [27]. This work expands towards higher spins earlier measurements of Ref. [28]. From the figure, it is clear that the alignment, which occurs in the two heavier Kr isotopes at a frequency $\hbar\omega \sim 0.45$ MeV, is delayed to a substantially higher frequency of ~ 0.8 MeV in ^{72}Kr . While it is tempting to assign this striking observation to the presence of an additional pairing contribution, caution is on order at this time. Indeed, other explanations, such as a change in deformation, can also account for the observation and it would be highly desirable to observe such an effect systematically in several $N = Z$ nuclei before a conclusion is reached. Preliminary Gammasphere results on ^{76}Sr and ^{80}Zr indicate that a similar delay in alignment may be present in these nuclei. If confirmed, the results presented here could then be viewed as an indication for $S=1$, $T=0$ pairing.

4.2. Superdeformation in ^{36}Ar

The microscopic description of collective motion is a fundamental challenge in quantum many-body physics. A classic example in the field of nuclear structure is the desire to un-

derstand within a spherical shell model framework the origins of nuclear deformation and collective rotation. Insight into this issue can be gleaned from comparisons between data, the results of deformed mean field calculations and rigorous shell model (SM) diagonalizations. The contradictory requirements of having a sufficiently large number of particles to develop rotation, and a sufficiently small number to permit SM calculations limits the opportunities for such direct comparisons. Considerable effort has been focussed recently on ^{48}Cr for this reason [29]. Because of the large shell gaps occurring at large deformation ($\epsilon_2 \sim 0.6$) for $N = Z = 18$, a superdeformed (SD) band in ^{36}Ar (associated with a configuration in which four particles are promoted to the pf shell) provides the opportunity to investigate a case involving cross-shell correlations characteristic of rotational motion in heavier nuclei (in the case of ^{48}Cr a single shell is involved). It is also noteworthy that the proton and neutron excitations involved are the same as those leading to deformation in the n-rich "island of inversion" around ^{32}Mg so that data on ^{36}Ar provide constraints on the effective interactions used in the SM calculations.

Using Gammasphere and Microball, a SD band in ^{36}Ar has recently been found with the $^{24}\text{Mg}(^{20}\text{Ne}, 2\alpha)$ reaction at 80 MeV by Svensson *et al.* [30]. A partial decay scheme is presented in Fig. 5: the band extends from the 2^+ level to the 16^+ state. Spin and parity assignments are based on angular distribution data for both the in-band and the linking transitions. Although absolute lifetime measurements have not been measured, the γ -ray branchings for the 4^+ and 6^+ states yield in-band to decay-out $B(E2)$ ratios consistent with the strongly enhanced transitions expected in a SD band. The inset in Fig. 5 compares the behavior of the SD band with data on the deformed band ($\epsilon_2 \sim 0.25$) in ^{48}Cr [29]. It can be seen that (i) up to the backbend, the rotational behavior in the ^{36}Ar band is even better than that of ^{48}Cr , and (ii) despite the considerable change in mass, the low-spin moments of inertia are comparable, implying a larger deformation and/or quenching of pairing correlations for ^{36}Ar . The maximum spin available in the $(s_{1/2}d_{3/2})^4(pf)^4$ configuration in ^{36}Ar is 16, and the high-energy γ ray from the 16^+ state suggests a band termination similar to that associated with the $(f_{7/2})^8$ configuration of ^{48}Cr .

In Ref. [30], extensive comparisons between cranked Nilsson-Strutinsky (CNS) calculations and large-scale $sp - df$ SM calculations with the code ANTOINE [31] are presented. As can be seen from the inset in Fig. 5, the SM calculations reproduce the data remarkably well and confirm the configuration assignment suggested by the CNS calculations. Given the success of both models in reproducing the data, a comparison of these complementary approaches is of interest. From such a comparison (see Ref. [30] for details) the following conclusions can be drawn: (1) the concept of a rotational band built on a fixed intrinsic state is validated by the calculated (spherical) subshell occupancies which are approximately constant up to $I \sim 10\hbar$; (2) the rapid variations in occupancies found at higher spin can be associated with the change in deformation of this intrinsic state from prolate to oblate; (3) for the pf -shell, the occupancy trends from the SM and CNS approaches are very similar; (4) quadrupole deformation effects can be largely accounted for by considering only the $f_{7/2}$ and $p_{3/2}$ orbitals, but the $f_{5/2}$ and $p_{1/2}$ orbitals lead to an important renormalization of the moment of inertia and are essential to obtain the agreement seen in Fig. 5. Finally, it was found that the quadrupole coherence available

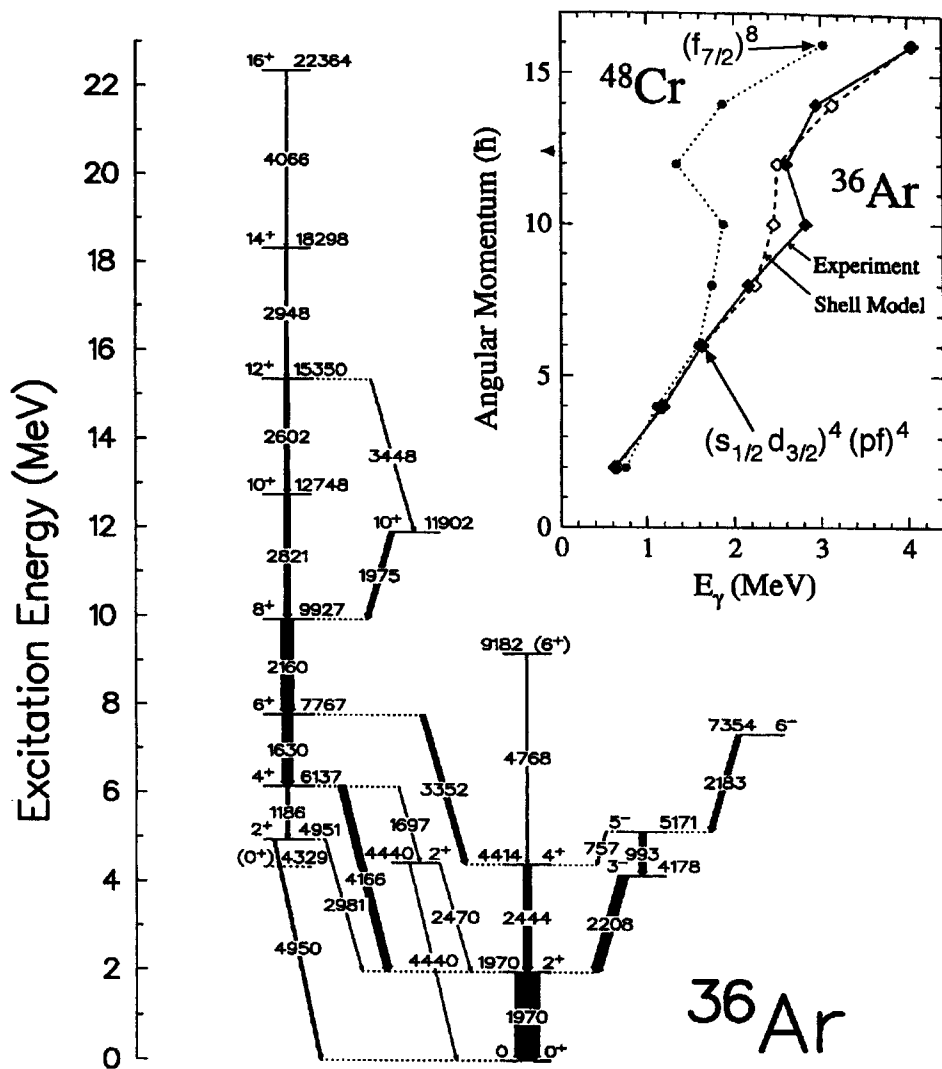


Figure 5. Level scheme for ^{36}Ar . The SD band is on the left. The inset presents the evolution of angular momentum with gamma-ray energy. A comparison with ^{48}Cr is indicated in the inset, as is a comparison with shell model calculations. Taken from Ref. [30].

which one would naively assume to be important for driving the shape, leads only to a modest increase in collectivity.

5. CONCLUSIONS

As stated above, Gammasphere was moved to the ATLAS facility with the aim of directing the power of the instrument towards exotic nuclei far from stability. The examples given above are only a few of those that can be used to illustrate the success of this Gammasphere campaign. At every step of our explorations of exotic nuclei, unexpected properties were uncovered such as the stability against fission of high-spin, high- Z nuclei, or the role of triaxiality in deformed proton emitters. First fingerprints for $S=1$, $T=0$ p-n pairing may have been found. The SD band of ^{36}Ar is not only the first experimental evidence for the eagerly anticipated superdeformation phenomenon in nuclei with mass $A\sim 40$, but is also an excellent opportunity to learn about the microscopic origins of collective motion in nuclei. These first attempts to study with a large array nuclei at the very limits of stability illustrate the point that many unexpected facets of the nuclear force remain to be discovered. At the dawn of the 21st century, there is promise for an exciting future in nuclear structure physics

6. ACKNOWLEDGMENTS

The author wishes to thank the many scientists who have provided the wonderful new ideas and challenges encountered during the Gammasphere campaign at ATLAS. They come from the world-wide nuclear physics community and are too numerous to be mentioned here by name. Special recognition is due to his colleagues at ANL, I. Ahmad, M.P. Carpenter, C. Davids, T. L. Khoo, F. G. Kondev, T. Lauritsen, C.J. Lister, D. Nisius, P. Reiter, D. Seweryniak, S. Siem, J. Uusitalo and I. Wiedenhöver, without whom the flawless operation of Gammasphere would not have been possible. This work is supported by the U.S. Department of Energy, Nuclear Physics Division, under Contract No. W-31-109-ENG-38.

REFERENCES

1. I. Y. Lee, Nucl. Phys. **A520**, (1990) 641c.
2. C. N. Davids *et al.*, Nucl. Instrum. Meth. Phys. Res. **B70**, (1992) 358.
3. Yu. Ts. Oganessian *et al.*, Nature (London) **400**, (1999) 242; Phys. Rev. Lett. **83**, (1999) 3154.
4. V. Ninov *et al.*, Phys. Rev. Lett. **83**, (1999) 1104.
5. S.G. Nilsson *et al.*, Nucl. Phys. **A115**, (1968) 545.
6. A. Sobiczewski, Phys. Part. Nuclei **25**, (1994) 119.
7. P. Reiter *et al.*, Phys. Rev. Lett. **82**, (1999) 509.
8. P. Reiter *et al.*, Phys. Rev. Lett. **84**, (2000) 3542.
9. Z. Patyl and A. Sobiczewski, Nucl. Phys. **A533**, (1991) 132; S. Cwiok *et al.*, Nucl. Phys. **A573**, (1994) 356; P. Moller *et al.*, At. Data Nucl. Data Tables **59**, (1995) 185.
10. S. Cwiok *et al.*, Nucl. Phys. **A611**, (1996) 211; W. Nazarewicz and P.-H. Heenen.

11. G. Lalazissis *et al.*, Nucl. Phys. **A608**, (1996) 202.
12. T. Duguet *et al.*, Nucl. Phys. *in press*.
13. J. L. Egido and L. M. Robledo, Phys. Rev. Lett. **85**, (2000) 1198.
14. I. Ahmad *et al.*, Phys. Rev. C **14**, (1976) 218.
15. F.P. Heßberger *et al.*, Z. Phys. **A359**, (1997) 415.
16. P. Ambruster, Proc. R.A. Welch Foundation, 41st Conf. on Chemical Research, Th Transactinide Elements, Houston, TX, p. 231.
17. P.J. Woods and C.N. Davids, Ann. Rev. Nucl. Part. Sci. **47**, (1997) 541.
18. C.N. Davids *et al.*, Phys. Rev. Lett. **80**, (1998) 1849; A.A. Sonzogni *et al.*, Phys. Rev. Lett. **83**, (1999) 1116.
19. D. Seweryniak *et al.*, to be published.
20. W. Nazarewicz *et al.*, Nucl. Phys. **A435**, (1985) 397.
21. S.M. Fischer *et al.*, Phys. Rev. Lett. **84**, (2000) 4064.
22. S.M. Fischer *et al.*, to be published.
23. W. Satula *et al.*, Phys. Lett. **B407**, (1997) 103.
24. A.L. Goodman *et al.*, Phys. Rev. C **60**, (1999) 014311; W. Satula and R. Wyss, Nucl. Phys. **A676**, (2000) 120, and references therein.
25. A. Algora *et al.*, Phys. Rev. C **61**, (2000) 031303R.
26. J. Becker *et al.*, Eur. Phys. Journ. **A4**, (1999) 103.
27. D.G. Sarantites *et al.*, Nucl. Inst. Meth. Phys. Res. **A381**, (1996) 418.
28. G. deAngelis *et al.*, Phys. Lett. **B415**, (1997) 217.
29. J.A. Cameron *et al.*, Phys. Lett. **B387**, (1990) 266; F. Brandolini *et al.*, Nucl. Phys. **A462**, (1998) 387 and references therein; K. Hara *et al.*, Phys. Rev. Lett. **83**, (1999) 1922, and references therein.
30. C.E. Svensson *et al.*, Phys. Rev. Lett. *in press*.
31. E. Caurier, computer code ANTOINE, IReS Strasbourg, (1989).